Numerical Analysis of SAR and Temperature Distribution in Human Eye Due to Moving Electromagnetic Source

Deepshikha Bhargava[1], and Phadungsak Rattanadecho[2*]

[1,2]Department of Mechanical Engineering, Faculty of Engineering, Thammasat University (Rangsit Campus), 99 moo 18, Klong Luang, Pathum Thani 12120, Thailand.

[*]E-mail: ratphadu@engr.tu.ac.th

Abstract

The study presents a numerical analysis of the absorption of electromagnetic (EM) radiation in human eye due to moving EM source. A two-dimensional eye model consisting of six types of tissues is exposed to a moving EM source operating at 900 and 1800 MHz frequencies for a time period of 10 minutes. Electric field intensity, specific absorption rate (SAR), and temperature distribution in the eye for both the frequencies have been calculated by solving a coupled model of electromagnetic wave and bio-heat transfer module. From the results it is concluded that the EM source's position, and the dielectric and thermal properties of the eye highly influence the absorption of EM radiation in the eye layers. SAR and temperature in the eye do not seem to correlate with each other. Effect of the size of the EM source on the EM absorption in the eye layers has also been investigated. The resultant SAR values in some cases exceeded the limited value whereas the temperature increase is found to be below the safety levels.

Keywords: Human eye, Moving EM source, Specific absorption rate, Temperature, FEM.

1. Introduction

Eyes are the most delicate part of our human body. Due to the absence of the outer skin layer and the lack of blood flow, they are more prone to the outer surroundings. Study of EM wave

interaction with the eye tissues has been a topic of interest for years. Temperature increase above some degrees in the eye is capable of causing thermal damage and adverse physiological effects in the tissues. Health organizations such as ICNIRP[1] and IEEE[2] have established limited EM exposure for the human body, measured in terms of specific absorption rate (SAR), where the main concern for the adverse effect in the eye has been the temperature increase in it. An increase of 3-4℃ temperature can cause cataract formation in the eye, where a temperature of 41℃ can cause posterior capsular opacities (PCO) [3-5]. Previous studies have shown formation of cataract in rabbit's eye after a 2-3 hours of exposure from microwave, whereas no cataract was formed in monkey's eye [6-8]. The study of heat transfer analysis in the human eye as a result of the exposure from EM wave is sparse. Most of the literature only discuses SAR [9-11], which is obvious considering that the safety guidelines are only based on it. However, in order to study the realistic situation and to get a better understanding of the phenomena, studying heat transfer analysis in the eye as a result of the EM radiation exposure is necessary.

Thermal analysis in the human eye has been discussed previously, Zarei et. al [12] studied the effect of sunglasses, with different ambient conditions, on the heat transfer in the eye and Firoozan et. al [13] studied the effect of different ambient conditions, convection coefficient etc. on the temperature increase in the eye to help control the eye temperature during the eye surgeries. Temperature increase due to EM radiation exposure has also been studied [14, 15], Bernardi et. al [15-17] included temperature distribution along with the SAR in the human body. They found that temperature and SAR in the eye do not correlate with each other and depend on the frequency of the EM radiation device. Lower frequency has higher wavelength which penetrates deeper into the tissue leading to higher temperature. However, For SAR, higher values were found at higher frequencies. Similar observation was made by Flyckt et. al [18],in their study they found higher

value of SAR in the deeper layers of the human eye model for higher frequency. In contrary to Bernardi et. al [15-17] findings, Hirata et. al [19, 20] in their study found SAR and temperature increase in the eye for plane and oblique incident waves to be corelating with each other.

Our lab has also been studying the SAR and temperature distribution in the human tissues as an exposure from EM radiation. Wesaapan et. al [5, 14, 21-23] have extensively studied effect of EM radiation on the SAR and temperature increase in the tissues such as eyes, body, head of adult and child, human genitals etc. Effect of metal objects such as jewelry and spectacles in proximity with the mobile phone radiation on the head and eye tissues has also been studied [24]. It has been concluded that studying temperature distribution along with SAR is important as factors like - type of the radiation source, position of the radiation source from the tissues, and the dielectric and thermal properties of tissues could influence the EM absorption leading to a noncorrelation between SAR and temperature.

In the literature, interaction of EM radiation with the eye has been studied when the EM source is in a stationary position. Meaning, the radiation has been incident on the eye from one direction and one position only. Situation when the EM source is continuously moving in front of the eye irradiating the larger region has not been discussed until now. This could be the case when a person gets exposed to some sort of moving EM radiation emitting device at places like industries, home etc. Some good example of it can be seen at convenience stores where the employees get exposed to the microwave radiation from the microwave oven several times throughout the day while standing and heating the food for their customers or a person on a video call keeps moving his hand and exposes the eyes to the mobile phone radiation in a continuous varying position, as shown in Fig 1. Hence, studying the case when eye gets exposed to a continuous moving EM source is important and could be useful for people who often find themselves in such situations.

Exposing the eye to a continuous moving EM source is somewhat similar to scanning a tissue. Some examples of continuous scanning of tissues can be seen in microwave imaging (MI) and laser therapy [25, 26]. In MI system, microwave emitting sources, like electrodes and antennas, are used to irradiate/scan the tissues at smaller-smaller portions one by one in order to construct an inside image of the tissues. Likewise, in laser therapy, the laser is projected on the skin on a smaller portion one by one. For scanning the eye (exposing it to a continuous moving source) a small EM radiation source needs to be created.

Continuous scanning has been performed by creating a gaussian function and using it as a moving source for scanning the tissue. Kabiri et. al [27] made a moving laser source using gaussian function and studied the effect of its velocity, intensity etc. on the temperature distribution in the skin and the kidney during the thermotherapy. Ma et. al [28] irradiate a three dimensional human tissue with a moving laser and studied the burn damage distribution on it. It was found that the size of the laser source and its speed highly influenced the thermal damage on the skin. Apart from this, pruet et. al [29] used a moving laser heat source to study its effect on the thermal behavior of the metal during the selective laser melting.

In this study, hence, a small EM radiation source, with the help of a gaussian function has been created for scanning the eye. The human eye is modelled in two-dimension consisting of seven types of tissues, shown in Fig.2. The EM radiation source operating at 900 and 1800 MHz frequencies takes 10 minutes to scan the whole eye area from the left side (Fig.3). Electric field, SAR and temperature distribution inside the eye as a result of the exposure from moving EM source at both frequencies are calculated. COMSOL™ Multiphysics software based on Finite Element Method (FEM) has been used for solving the coupled model of EM wave propagation (TE mode) and bio-heat transfer analysis. Maxwell's equations are used to solve the EM wave

propagation analysis inside the tissues as well as in its surrounding area [14, 30]. Whereas, classical heat conduction equation is used to solve the heat transfer analysis in the tissues [19, 31, 32]. The effect of the size of EM radiation source on the SAR and temperature increase in the eye has also been discussed.

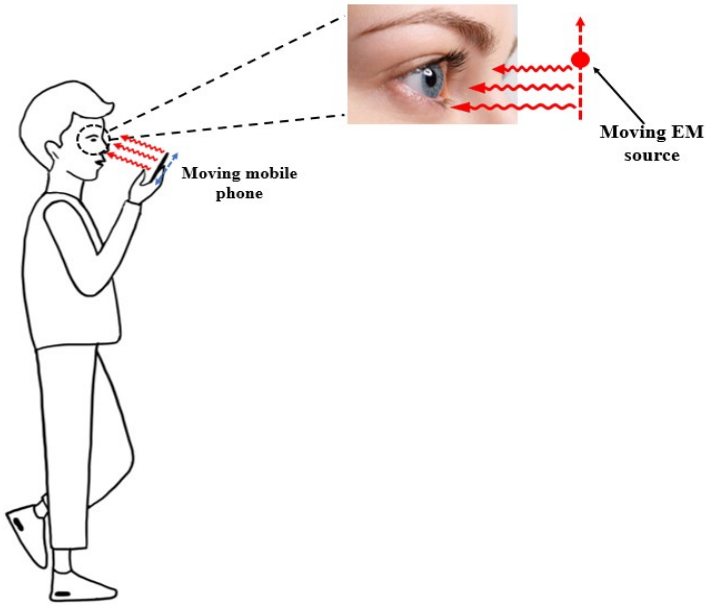

Fig.1 Human eye exposed to the moving EM source.

2. Problem Formulation

2.1 Physical Model

EM absorption in a human eye as a result of the exposure from moving EM source is studied (Fig.1). A two-dimensional eye model is created to study the EM wave and heat transfer analysis in the eye tissues as a result of the exposure from moving EM source, shown in Fig.2. This eye model has previously been used by Shafahi and Vafai [33]. The eye model consists of seven types of tissues namely posterior chamber, vitreous, sclera, lens, cornea, anterior chamber, and iris. The

dielectric and thermal properties of the tissues are taken from Table 1 and 2, respectively. In this study, sclera and iris are considered as one homogenous tissue, hence, they have the same properties. An EM radiation source of size 5 mm, operating at 900 and 1800 MHz frequencies and at 1000Watt power is created and scanned on the left side of the eye model with the help of gaussian function (Fig.3). The radiated power is chosen considering an extreme/worst case. Situation when a person may get exposed to poor-quality devices which radiates more power. Continuous exposure of these bad quality devices may cause harmful effect on the eye. Hence, an EM source radiating at 1000W power is considered for this study. The EM source moves on a port boundary of 3 cm and scans the whole eye in 10 minutes. The EM absorption and the temperature in the eye as a result of EM exposure are calculated using COMSOL^{TM} Multiphysics software based on FEM.

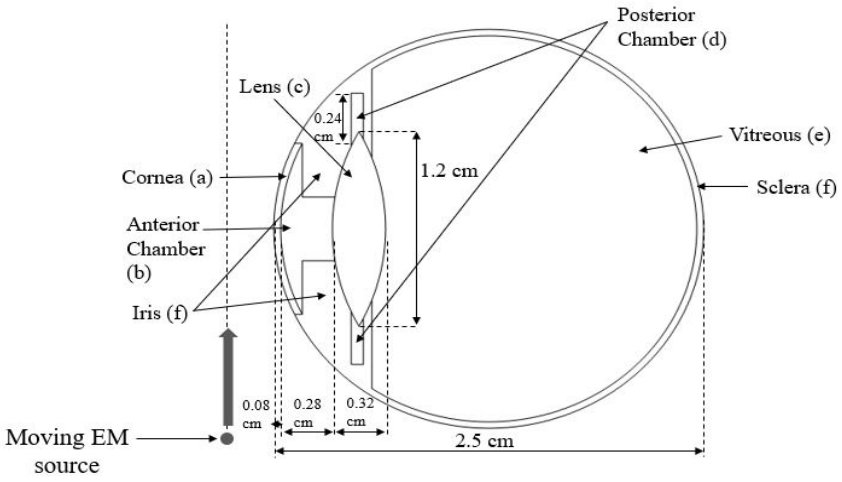

Fig.2 Physical model of human eye

Table 1 Dielectric properties of eye tissues at different frequencies [15, 34]

Tissue	Frequency: 900 MHz		Frequency: 1800 MHz	
	ε_r	σ (S/m)	ε_r	σ (S/m)
Cornea (a)	52.00	1.85	55.0	2.32
Anterior Chamber (b)	73.00	1.97	75.0	2.40
Lens (c)	51.30	0.89	41.1	1.29
Posterior Chamber (d)	73.00	1.97	75.0	2.40
Vitreous (e)	74.30	1.97	73.7	2.33
Sclera (f)	52.10	1.22	52.7	1.68
Iris (f)	52.10	1.22	52.7	1.68

Table 2 Thermal properties of eye tissues [35]

Tissue	ρ(kg/m^3)	k (W/°C)	C_p(J/kg°C)
Cornea (a)	1050	0.58	4178
Anterior Chamber (b)	996	0.58	3997
Lens (c)	1000	0.4	3000
Posterior Chamber (d)	996	0.58	3997
Vitreous (e)	1100	0.603	4178
Sclera (f)	1050	1.0042	3180
Iris (f)	1050	1.0042	3180

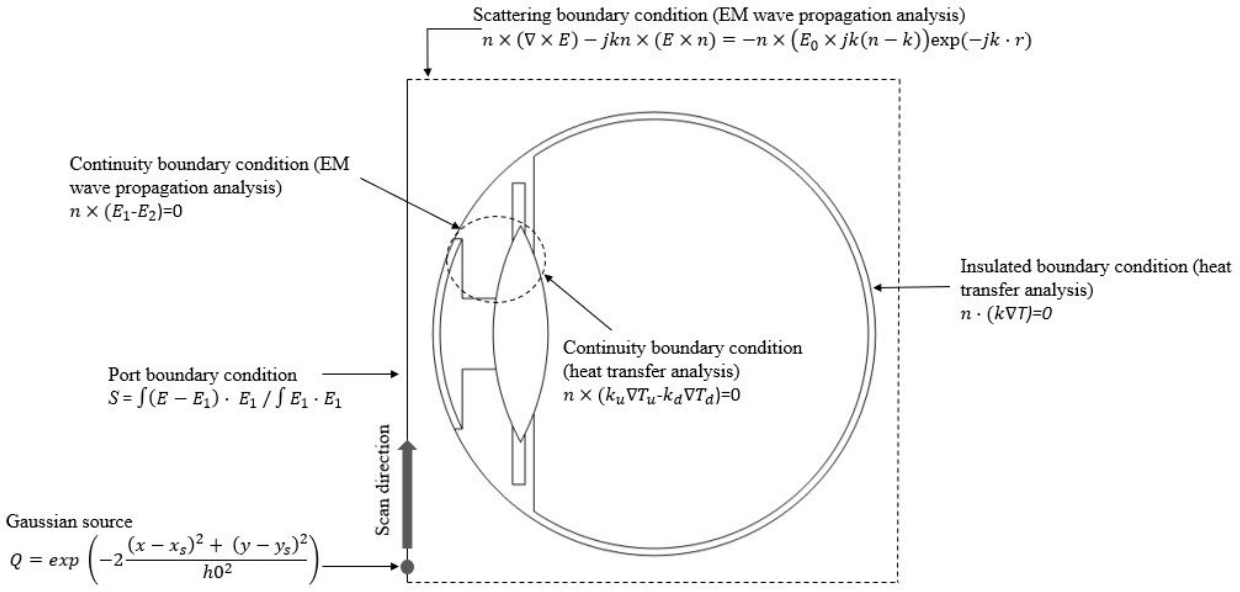

Fig. 3 Boundary condition for electromagnetic wave propagation and bio-heat transfer analysis.

2.2 Equations for Electromagnetic wave propagation analysis

The EM radiation source moves continuously in the upward direction irradiating the eye. The EM wave propagation, inside the eye tissues and in the surroundings, is numerically solved using Maxwell's equations. In order to reduce the computation time while not compromising with the results, the analysis has been carefully performed in two-dimension. To further simplify the calculation of EM wave propagation analysis, following assumptions are made [5] -

1. The EM wave propagate and interacts with the eye tissues in two dimensions.

2. The Eye model surroundings are truncated using scattering boundary condition.

3. The dielectric properties of the eye tissues are uniform and constant throughout the calculations.

4. The propagation of EM wave is in Transverse Electric mode (TE mode).

The EM wave propagation in the free space and through the eye tissues are solved using

Maxwell's equation in TE mode-

$$\nabla \times \left(\frac{1}{\mu_r}\nabla \times E\right) - k_0^2\left(\varepsilon_r - \frac{j\sigma}{\omega\varepsilon_0}\right)E = 0 \quad (1)$$

where E is Electric field (V/m), μ_r is the relative magnetic permeability, ε_r is the relative dielectric constant, ε_0 = 8.8542× 10^{-12}F/m is the permittivity of free space, σ is the electrical conductivity (S/m), and k_0 is the free space wave number (m^{-1}).

2.2.1 Boundary condition for wave propagation analysis

Port boundary condition is applied on the outer region of the left side of the model, as shown in Fig. 3. The port emits EM wave in TE mode at 1000-Watt power.

$$S = \frac{\int(E-E_1)\cdot E_1}{\int E_1 \cdot E_1} \quad (2)$$

Continuity boundary condition is applied between air and eye model and in between the eye tissues-

$$n \times (H_1 - H_2) = 0 \quad (3)$$

The area outside the eye model is truncated using the scattering boundary condition –

$$n \times (\nabla \times E_z) - jkE_z - jkE_z = -jk(1 - k \cdot n)E_{0z}\exp(-jk \cdot r) \quad (4)$$

where k is the wave number (m^{-1}), σ is the electric conductivity (S/m), n is normal vector, j = $\sqrt{-1}$, and $E_0$is the incident plane wave (V/m).

2.2.2 moving source

[29]A gaussian function is created on the port boundary condition acting as an EM radiation source, moving in the upward direction as shown in Fig 3. The gaussian function takes total 10 minutes to cover the port. The size of the gaussian function with its movement in the upward

direction on the port is expressed as Eq. (5).

$$Q = \exp\left(-2\frac{(x-x_s)^2+(y-y_s)^2}{h0^2}\right) \quad (5)$$

where, x_s and y_s are the horizontal and vertical positions of the source in x and y directions, respectively, and h_0 is the height of the source, The EM source moves only in the y direction, hence the movement in the x position stays the same.

2.3 Interaction of Electromagnetic wave with human tissues

The EM wave propagates in free space, incident on the eye and gets absorbed by the eye tissues. This absorbed energy is known as specific absorption rate (SAR). The SAR in the eye tissues are calculated and can be expressed as [5, 14] –

$$SAR = \frac{\sigma}{\rho}|E|^2 \quad (6)$$

where E is the electric field intensity (V/m), σ is the electric conductivity (S/m), and ρ is the tissue density.

2.4 Equation for heat transfer analysis

The temperature distribution inside the eye tissues is studied using classical heat conduction equation. The initial temperature of the eye model is set to 37°C. For simplifying the thermal analysis, following assumption are made[5] -

1. The thermal properties of the eye tissues remain constant and uniform.
2. The tissues are biomaterial.
3. There is no energy exchange, phase change, and chemical reaction occurring in the tissues.

[12]Classical heat conduction equation is used to calculate the temperature distribution in the tissues, shown in Eq. (7). The transient equation is capable of effectively analyzing the heat transfer

occurring in the tissues-

$$\rho C \frac{\partial T}{\partial t} = \nabla \cdot (k \nabla T) + Q_{ext} \quad (7)$$

where ρ is the tissue density (kg/m^3), C is the heat capacity of tissue (J/kg °C), k is the thermal conductivity of tissue (W/m °C), T is the tissue temperature (°C), and Q_{ext} is the external heat source term (electromagnetic heat-source density) (W/m^3).

Q_{ext} is the external heat source term equal to the resistive heat generated by electromagnetic field (electromagnetic power absorbed), defined as [5]-

$$Q_{ext} = \frac{1}{2} \sigma_{tissue} |E|^2 = \frac{\rho}{2} \cdot SAR \quad (8)$$

2.4.1 Boundary condition for heat transfer analysis

An insulated boundary condition is applied on the outer surface of the eye model to isolate it from the surroundings as the heat transfer analysis is only considered within the eye-

$$n \cdot (k \nabla T) = 0 \quad (9)$$

Continuity boundary condition is applied between the eye layers showing there is no contact resistance between them-

$$\nabla T_u = \nabla T_d \quad (10)$$

$$n \cdot (k_u \nabla T_u - k_d \nabla T_d) = 0 \quad (11)$$

2.5 Numerical method

FEM is used to calculate the SAR and temperature in the eye tissues as a result of the exposure from moving EM source. The first step of FEM is to divide the geometry in several small parts of different shapes called meshing, shown in Fig. 4. The coupled model of EM wave and bioheat transfer are then solved numerically. The numerical analysis is performed on each part of the mesh in order to get the precise results. To make sure that the obtained results are independent of the number of mesh elements, a mesh convergence test is performed. Fig.5 shows the graph between the number of mesh elements and the temperature in the cornea layer of the eye. The analysis is performed for 1800 MHz frequency when the EM source is at 317 sec position. As can be seen after 2865 number of mesh elements the value of temperature becomes consistent. This shows that the obtained results after that certain number of mesh elements become independent of the mesh elements. At this point it is fair to assume that the results are reliable and precise.

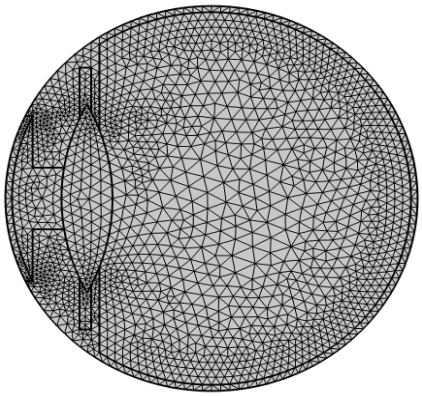

Fig. 4 Two-dimension mesh model of human eye

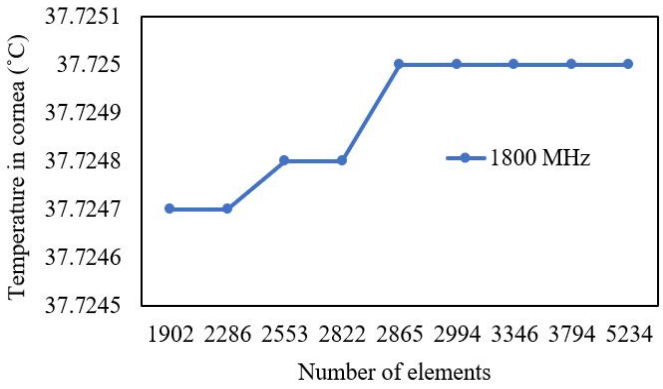

Fig.5 Grid convergence graph between number of mesh elements and temperature.

3. Results and discussions

3.1 Numerical validation

The proposed numerical model is verified by comparing the temperature distribution obtained in the eye model without the electromagnetic module with the results of Shafahi and Vafai [33]. It is to be noted that the comparison has been made for the static EM source, since it is really difficult to find a similar case in the literature. The heat transfer coefficient and ambient temperature for the verification model are assumed 20 W/m^{2}K and 25˚C, respectively. As can be seen, the obtained temperature in the eye along the pupillary axis is almost similar to the results from Shafahi and Vafai [33] as shown in Fig. 6. This favorable agreement between the two studies provides credence to the proposed model.

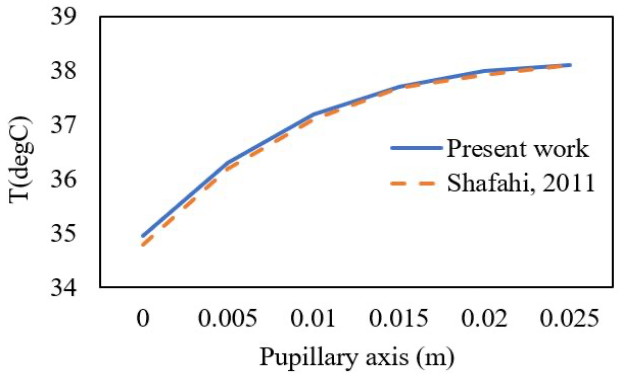

Fig.6 Comparison of the temperature distribution inside the eye between present work and the work of Shafahi and Vafai [33].

3.2 Electric field intensity inside the eye

The EM radiation source moves on the port boundary of the model (Fig. 3) and scans the eye from the left side. The length of the port boundary is 3 cm and the size of the EM radiation source is 5 mm. The EM source is in TE mode, operating at 900 and 1800 MHz frequencies with 1000 W power. The EM source takes 10 minutes to move across the port boundary. Fig. 7 shows the EM source positions at 0, 100, 200, 300, 400, 500, and 600 seconds. The electric fields propagate from the EM source through free space and incident on the eye where the tissues absorb it. Fig. 8 shows the electric field distribution in the eye at 0, 317, and 600 seconds for 900 and 1800 MHz frequencies. As can be seen the highest value of electric field intensity in the eye is found when the EM source has travelled 317 seconds and is now at a position very close to the eye. At this point of time, for both frequencies, the highest value of EM absorption in the eye has been found in the cornea layer. Whereas, at 0 sec and 600 sec it is highest in the sclera layer. Cornea and sclera being the outermost layer of the eye and closer to the EM source gets more exposed. Hence, more absorption of the EM radiation in these layers. The EM distribution then diminishes as it goes deeper into the eye layers. Highest value of EM intensities at 0 sec (14.57 V/m) and 600 sec (15.40 V/m) are found for 900 MHz frequency. Whereas, for 317 sec (164.91 V/m) it is found for 1800 MHz frequency. Dielectric properties mentioned in Table 1 plays an important part in the EM absorption in the layers. The lower ε_r values of cornea and sclera when used in Eq. (1) causes easier penetration in the layers leading to higher values of electric field intensity. This absorbed energy in the layers then converts into the heat. Section 3.3 and 3.4 discusses the SAR and temperature distribution in the eye layers as a result of the absorption of EM field.

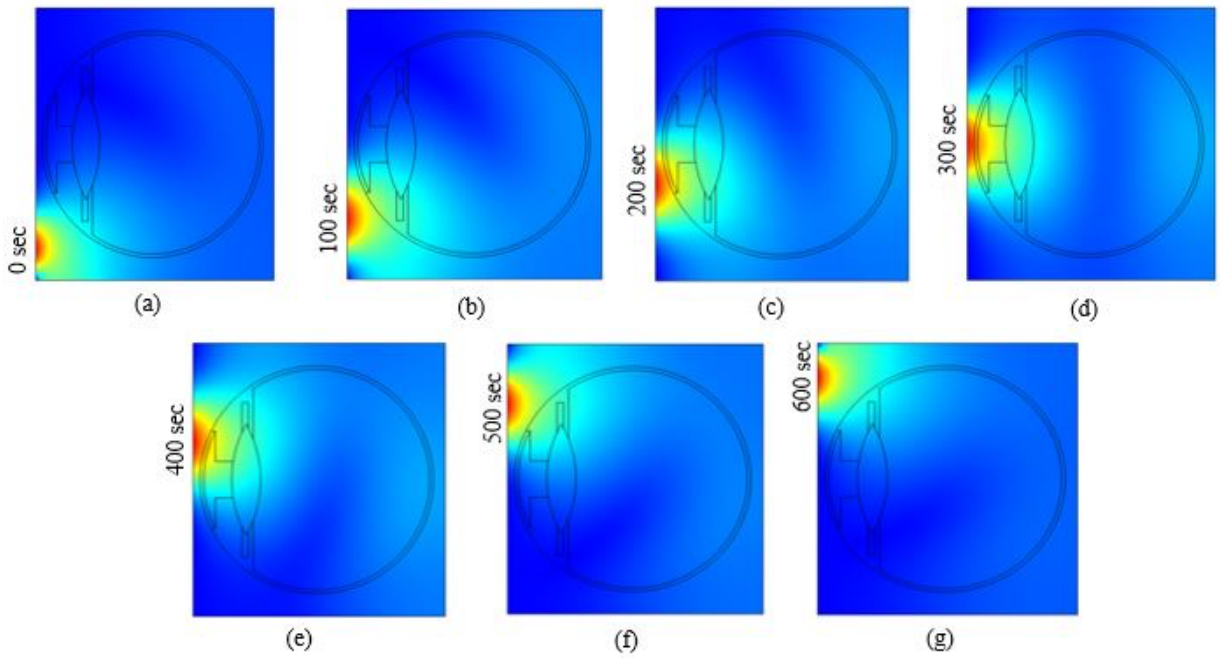

Fig.7 Moving electromagnetic source positions from 0 to 600 seconds.

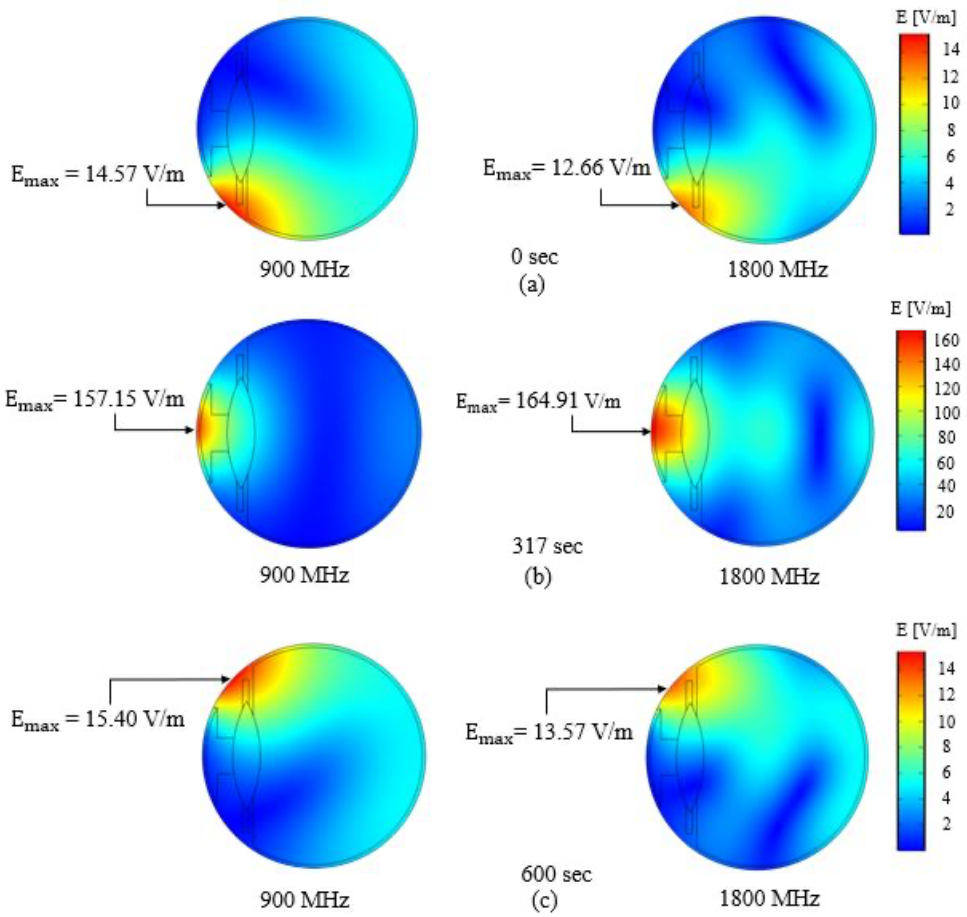

Fig.8 Electric field distribution in the eye at (a) 0 sec, (b) 317 sec, and (c) 600 sec.

3.3 SAR distribution inside the eye

Fig. 9 shows the SAR distribution in the eye layers as a result of the exposure from moving EM source at 900 and 1800 MHz frequencies. It is observed, following the electric field intensity (section 3.2), the highest value of SAR in the eye has also been found in the cornea layer of the eye at 317 sec for 1800 MHz frequency. However, at 0 sec and 600 sec it is found highest in the posterior chamber. The dielectric properties (σ, Table 1) and thermal properties (ρ, Table 2) plays an important role in calculating the SAR in the eye layers. The lower value of ρ in the posterior chamber than the sclera and higher value of σ in the posterior chamber than the sclera lead to higher value of SAR in the posterior chamber (Eq.6). Highest value of SARs at 0 sec (0.17 W/kg) and 600 sec (0.19 W/kg) are found for 900 MHz frequency. Whereas for 317 sec (31.54 W/kg) it is found for 1800 MHz frequency. Considering the ICNIRP limits of 2 W/kg (general public exposure) and 10 W/kg (occupational exposure) for EM exposure, the SAR values obtained in the cornea at 317 sec exceeds the ICNIRP threshold values. This calculated SAR values are then used to calculate the temperature distribution inside the eye layers (section 3.4).

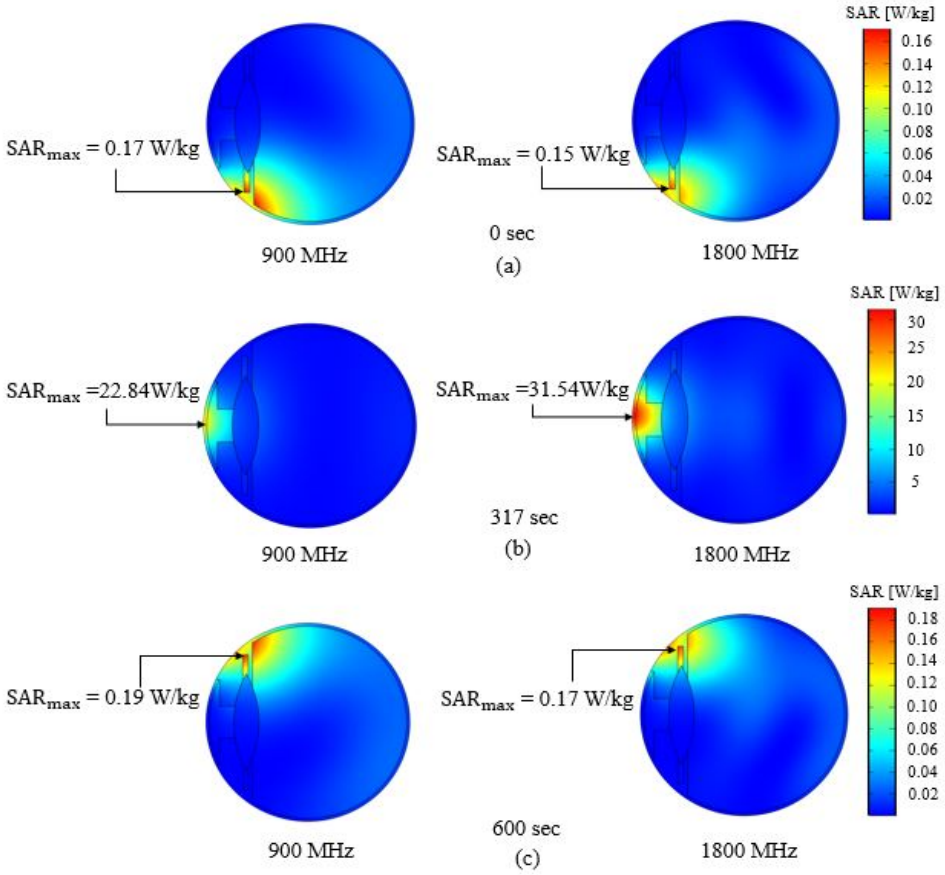

Fig.9 SAR distribution in the eye at (a) 0 sec, (b) 317 sec, and (c) 600 sec.

3.4 Temperature inside the eye

The temperature distribution inside the eye layers as a result of the exposure from EM radiation is calculated. A coupled model of electromagnetic wave propagation and bioheat transfer is solved numerically. The electric field intensity (Fig.8) and SAR (Fig.9) in the eye now converts into thermal energy leading to temperature increase. Fig.10 shows the temperature distribution in the eye at three-time instants 0 sec, 317 sec, and 600 sec for 900 and 1800 MHz frequencies. Initial temperature in the eye has been set to 37˚C. The electromagnetic source moves across the port boundary and irradiate the eye. The electromagnetic energy is then absorbed by the eye tissues. This absorbed energy in the tissues then transforms into heat increasing the overall temperature in the eye. At 0 sec, for both the frequencies, the maximum temperature in the eye is equal to the initial temperature. At 317 sec, the maximum temperature is found in the cornea layer of the eye for 1800 MHz frequency. Which is similar to electric field intensity and SAR distribution in the eye. However, at 600 sec, the maximum temperature in the eye is still in the cornea layer for 1800 MHz frequency. Which is different than the electric field intensity and the SAR distribution cases. The maximum value of temperature at 0 sec is 37.0 ˚C, at 317 sec is 37.72 ˚C, and at 600 sec is 37.44 ˚C. It is observed that the thermal properties from Table 2, highly influenced the temperature increase in the eye. However, this temperature increase is still very low to cause any harmful effect.

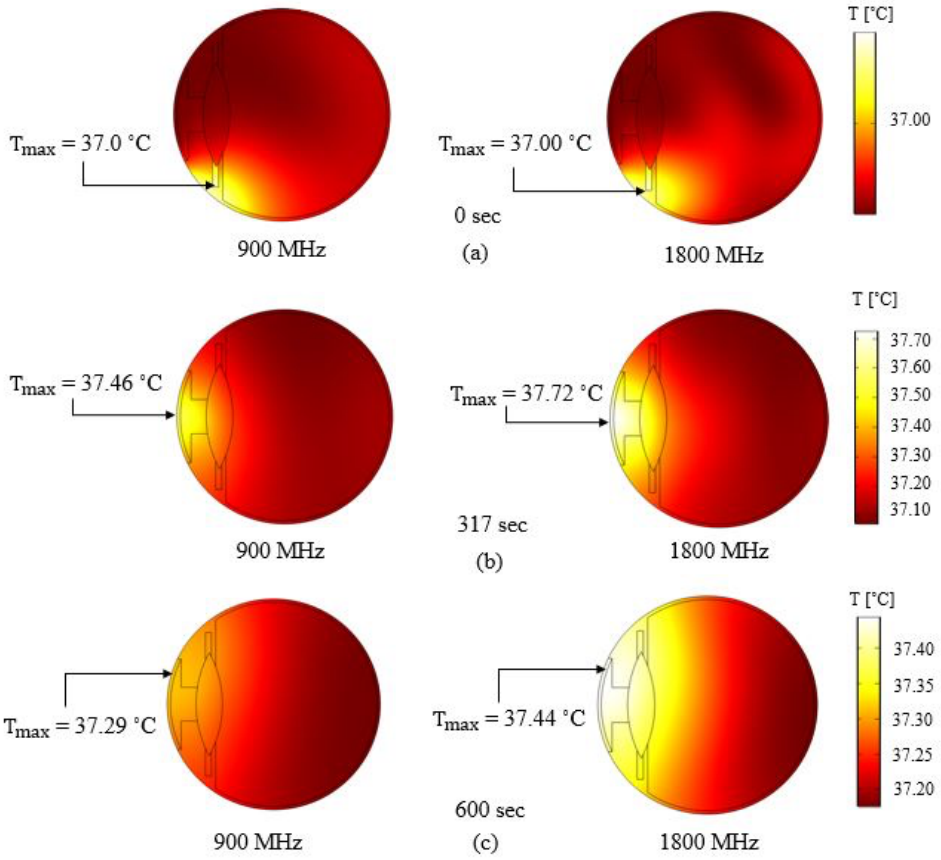

Fig.10 Temperature distribution in the eye at (a) 0 sec, (b) 317 sec, and (c) 600 sec

3.5 Effect of the size of EM source

Effect of different sizes of EM source on the SAR and temperature distribution in the eye has also been studied. Five sizes from 1 to 5mm are chosen for the EM source. Comparison of SAR at both frequencies for different sizes of EM sources has been performed, shown in Fig. 11. The comparison has only been shown for the 317 sec position, as this is where the maximum absorption of EM energy in the eye is found. It can be seen from the results that the EM energy absorption in the eye is directly proportional to the size of the source. Larger the size of the EM source higher the SAR value in the eye. Smaller size EM source has low absorption and low penetration depth in the eye. It has also been observed that 1800 MHz frequency causes more absorption and penetration in the eye in comparison to 900 MHz frequency. This is because the dielectric properties of eye at 1800 MHz frequency are significantly higher than 900 MHz frequency (Table 1). The higher electrical conductivity and permittivity cause more absorption, Eq. (6). The temperature distribution in the eye follows the SAR distribution, shown in Fig. 12. Just like SAR, higher value of temperature is found for the larger size of EM source. Also, 1800 MHz frequency showed more absorption and penetration depth of temperature in comparison to the 900 MHz. Higher value of SAR at 1800 MHz in comparison to 900 MHz causes higher value of temperature at 1800 MHz according to Eq. (7) and (8). By comparing the SAR and temperature in the eye as a result of different sizes of EM source with the safety guidelines, it is concluded that the SAR values at all sizes exceeded the ICNIRP limit of 2 W/kg. However, the temperature increase in the eye has still found to be low to cause any serious adverse effect on the eye [3, 4].

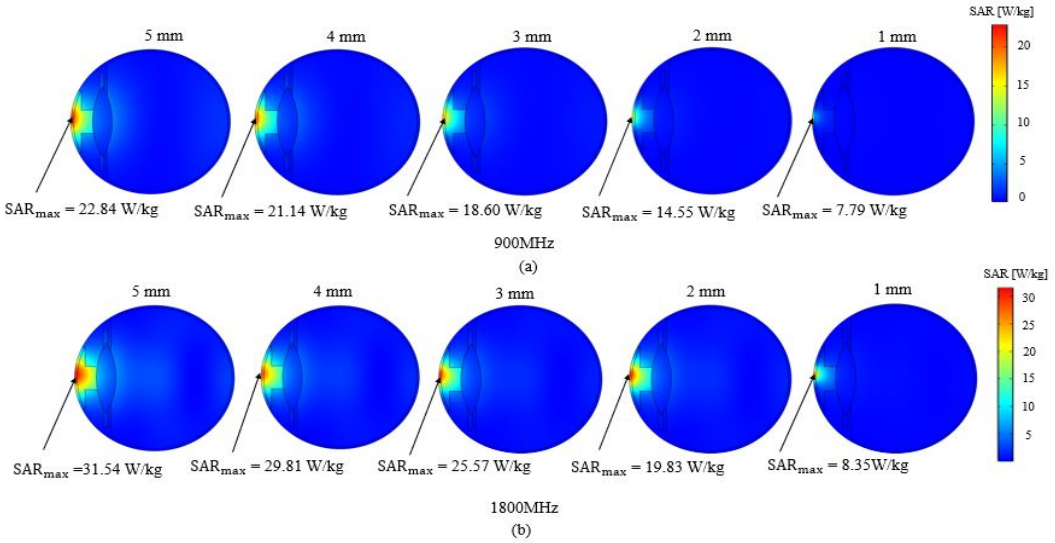

Fig. 11 Comparison of different sizes of EM source on the SAR in the eye at 317 sec position for (a) 900 MHz, and (b) 1800 MHz frequencies.

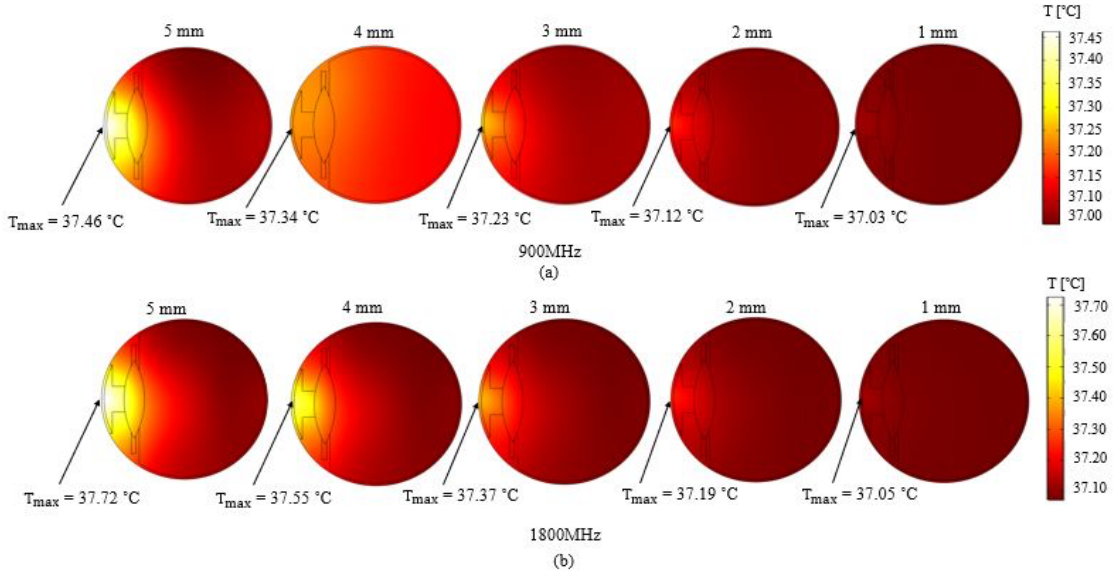

Fig. 12 Comparison of different sizes of EM source on the temperature in the eye at 317 sec position for (a) 900 MHz, and (b) 1800 MHz frequencies.

4. Conclusion

This study presents the absorption of EM radiation in a two-dimensional human eye model as a result of the exposure from moving EM source propagating in TE mode at 900 and 1800 MHz frequencies with 1000 W power. The EM source takes total 10 minutes to move across the port and irradiate the eye from the left side. The results showed that the maximum value of EM energy absorption occurs when the source is at 317 sec. This is the position when the distance between the EM source and the eye is smallest which leads to higher EM absorption in the eye. Maximum value of electric field intensity, SAR and temperature are found in the cornea layer of the eye at 317 sec position for 1800 MHz frequency. This is because cornea is the outermost layer of the eye, at 317 sec position of EM source, it gets more exposed in comparison to the other layers of the eye. Also, the dielectric properties of the eye at 1800 MHz frequency is higher than the 900 MHz frequency. This leads to more absorption of EM energy and SAR at 1800 MHz frequency which causes higher temperature. For 0 sec position, the maximum value of electric field intensity is found in sclera layer (14.57 V/m at 900 MHz), maximum SAR is found in posterior chamber (0.17 W/kg at 900 MHz), and temperature is same for all layers (37.0 ˚C). For 600 sec, the maximum value of electric field intensity is found in sclera layer (15.40 V/m at 900 MHz), maximum value of SAR in posterior chamber (0.19 W/kg at 900 MHz), and maximum temperature in cornea layer (37.44˚C at 1800 MHz). For 317 sec position, the maximum value of electric field intensity is found in cornea layer (164.91 V/m at 1800MHz), maximum value of SAR is also found in cornea layer (31.54 W/kg at 1800 MHz), and maximum temperature is also found in the cornea layer (37.72˚C at 1800 MHz). Effect of different sizes of EM sources on the SAR and temperature distribution in the eye has also been studied. It was found that larger size of the EM source causes higher energy absorption in the eye. In all cases at 317 sec, the SAR value in the eye exceeded the

limited exposure values. However, the temperature value in the eye is still below the threshold value to cause any adverse effect.

Acknowledgment

This study was supported by the Thammasat Postdoctoral Fellowship and Program Management Unit for Human Resources & Institutional Development, Research, and Innovation, NXPO (Grant Number B05F630092, B05F640205), National Research Council of Thailand (Grant Number N42A650197). Thailand Science Research and Innovation Fundamental Fund (Project No. 66082).

Conflict of Interest

There are no conflicts to declare.

Reference

[1] ICNIRP, *Health Phys,* 2020,**118**, 483-524, doi: 10.1097/hp.0000000000001210.

[2] IEEE, *IEEE Std C95.1-2019 (Revision of IEEE Std C95.1-2005/ Incorporates IEEE Std C95.1-2019/Cor 1-2019),* 2019, 1-312, doi: 10.1109/IEEESTD.2019.8859679.

[3] J. C. Lin, *IEEE Antennas Propag. Mag.,* 2003,**45**, 171-174, doi: 10.1109/MAP.2003.1189664.

[4] C. Buccella, V. D. Santis, M. Feliziani, *IEEE Trans. Electromagn. Compat.,* 2007,**49**, 825-833, doi: 10.1109/TEMC.2007.909024.

[5] T. Wessapan, P. Rattanadecho, *J. Heat. Transf.,* 2012,**134**, 091101-091111, doi: 10.1115/1.4006243.

[6] A. W. Guy, J. C. Lin, P. O. Kramar, A. F. Emery, *IEEE Trans. Microw. Theory Tech.,*

1975,**23**, 492-498, doi: 10.1109/TMTT.1975.1128606.

[7] P. Kramar, C. Harris, A. F. Emery, A. W. Guy, *J Microw Power,* 1978,**13**, 239-249, doi: 10.1080/16070658.1978.11689101.

[8] Y. Kamimura, K.-i. Saito, T. Saiga, Y. Amemiya, *IEICE Trans. Commun,* 1994,**77**, 762-765,doi:https://search.ieice.org/bin/summary.php?id=e77b_6_762&category=B&year=1994&lang=E&abst=.

[9] O. P. Gandhi, G. Lazzi, C. M. Furse, *IEEE Trans. Microw. Theory Tech.,* 1996,**44**, 1884-1897, doi: 10.1109/22.539947.

[10] O. Fujiwara, A. Kato, *IEICE Trans. Commun,* 1994,**77**, 732-737, doi: https://search.ieice.org/bin/summary.php?id=e77b_6_732&category=B&year=1994&lang=E&abst=.

[11] J. Q. Lan, X. Liang, T. Hong, G. H. Du, *Prog. Biophys. Mol. Biol.,* 2018,**136**, 29-36, doi: https://doi.org/10.1016/j.pbiomolbio.2018.02.001.

[12] K. Zarei, M. Lahonian, S. Aminian, S. Saedi, M. Ashjaee, *J. Therm. Biol.,* 2021,**99**, 102971, doi: 10.1016/j.jtherbio.2021.102971.

[13] M. S. Firoozan, S. Porkhial, A. S. Nejad, *J Therm Biol,* 2015,**47**, 51-58, doi: 10.1016/j.jtherbio.2014.11.001.

[14] D. Bhargava, N. Leeprechanon, P. Rattanadecho, T. Wessapan, *Int. J. Heat Mass Transf.,* 2019,**130**, 1178-1188, doi: https://doi.org/10.1016/j.ijheatmasstransfer.2018.11.031.

[15] P. Bernardi, M. Cavagnaro, S. Pisa, E. Piuzzi, *IEEE Trans. Microw. Theory Tech.,* 2000,**48**, 1118-1126, doi: 10.1109/22.848494.

[16] P. Bernardi, M. Cavagnaro, S. Pisa, E. Piuzzi, *IEEE Trans. Microw. Theory Tech.,* 1998,**46**, 2074-2082, 10.1109/22.739285.

[17] P. Bernardi, M. Cavagnaro, S. Pisa, E. Piuzzi, *IEEE Trans Biomed Eng,* 2003,**50**, 295-304, doi: 10.1109/TBME.2003.808809.

[18] V. M. M. Flyckt, B. W. Raaymakers, H. Kroeze, J. J. W. Lagendijk, *Phys. Med. Biol.,* 2007,**52**, 2691, doi: 10.1088/0031-9155/52/10/004.

[19] A. Hirata, S. Matsuyama, T. Shiozawa, *IEEE Trans. Electromagn. Compat.,* 2000,**42**, 386-393, doi: 10.1109/15.902308.

[20] A. Hirata, H. Watanabe, T. Shiozawa, *IEEE Trans. Electromagn. Compat.,* 2002,**44**, 592-594, doi: 10.1109/TEMC.2002.804778.

[21] T. Wessapan, P. Rattanadecho, *Journal of Medical and Bioengineering* 2014 **3**, 251-258, doi:http://www.phadungsak.me.engr.tu.ac.th/downloads/2014%20Journal%20of%20Medical%20and%20Bioengineering.pdf.

[22] T. Wessapan, P. Rattanadecho, *Int. J. Heat Mass Transf.,* 2018,**119**, 65-76, doi: https://doi.org/10.1016/j.ijheatmasstransfer.2017.11.088.

[23] T. Wessapan, S. Srisawatdhisukul, P. Rattanadecho, *Int. J. Heat Mass Transf.,* 2012,**55**, 347-359, doi: https://doi.org/10.1016/j.ijheatmasstransfer.2011.09.027.

[24] D. Bhargava, P. Rattanadecho, T. Wessapan, *Case Stud. Therm. Eng.,* 2020,**22**, 100789, doi: https://doi.org/10.1016/j.csite.2020.100789.

[25] R. Inum, M. M. Rana, K. N. Shushama, M. A. Quader, *Int. J. Biomed. Imaging,* 2018,**2018**, 1-12, doi: 10.1155/2018/8241438.

[26] J. Ma, X. Yang, S. Liu, Y. Sun, J. Yang, *Int. J. Heat Mass Transf.,* 2018,**124**, 1107-1116, doi: https://doi.org/10.1016/j.ijheatmasstransfer.2018.04.042.

[27] A. Kabiri, M. R. Talaee, *Lasers Med Sci.,* 2021,**36**, 583-597, doi: 10.1007/s10103-020-03070-7.

[28] J. Ma, X. Yang, Y. Sun, J. Yang, *Sci. Rep.,* 2019,**9**, 10987, doi: 10.1038/s41598-019-47435-7.

[29] P. Ninpetch, P. Kowitwarangkul, S. Mahathanabodee, P. Chalermkarnnon, P. Rattanadecho, *Case Stud. Therm. Eng.,* 2021,**24**, 100860, doi: https://doi.org/10.1016/j.csite.2021.100860.

[30] J. W. Hand, *Phys. Med. Biol.,* 2008,**53**, R243, doi: 10.1088/0031-9155/53/16/R01.

[31] J. A. Scott, *Physics in Medicine and Biology,* 1988,**33**, 227-242, doi: 10.1088/0031-9155/33/2/003.

[32] E. H. Amara, *Int. J. Heat Mass Transf.,* 1995,**38**, 2479-2488, doi: https://doi.org/10.1016/0017-9310(94)00353-W.

[33] M. Shafahi, K. Vafai, *J. Heat. Transf.,* 2010,**133**, doi: 10.1115/1.4002360.

[34] P. Sooman, J. Juyoung, L. Yeongseog, *ICMMT 4th International Conference on, Proceedings Microwave and Millimeter Wave Technology, 2004.,* 2004, 966-969, doi: 10.1109/ICMMT.2004.1411692.

[35] E. H. Ooi, E. Y. Ng, *Comput Biol Med,* 2008,**38**, 252-262, doi: 10.1016/j.compbiomed.2007.10.007.

